

Hyperparameter Tuning in Echo State Networks

Filip Matzner

filip.matzner@mff.cuni.cz

Charles University

Faculty of Mathematics and Physics

Prague, Czech Republic

ABSTRACT

Echo State Networks represent a type of recurrent neural network with a large randomly generated reservoir and a small number of readout connections trained via linear regression. The most common topology of the reservoir is a fully connected network of up to thousands of neurons. Over the years, researchers have introduced a variety of alternative reservoir topologies, such as a circular network or a linear path of connections. When comparing the performance of different topologies or other architectural changes, it is necessary to tune the hyperparameters for each of the topologies separately since their properties may significantly differ. The hyperparameter tuning is usually carried out manually by selecting the best performing set of parameters from a sparse grid of predefined combinations. Unfortunately, this approach may lead to underperforming configurations, especially for sensitive topologies. We propose an alternative approach of hyperparameter tuning based on the Covariance Matrix Adaptation Evolution Strategy (CMA-ES). Using this approach, we have improved multiple topology comparison results by orders of magnitude suggesting that topology alone does not play as important role as properly tuned hyperparameters.

CCS CONCEPTS

• **Computing methodologies** → *Neural networks*; • **Theory of computation** → *Evolutionary algorithms*; **Continuous optimization**.

KEYWORDS

echo state networks, evolution strategies, parameter tuning, continuous optimization

ACM Reference Format:

Filip Matzner. 2022. Hyperparameter Tuning in Echo State Networks. In *Genetic and Evolutionary Computation Conference (GECCO '22)*, July 9–13, 2022, Boston, MA, USA. ACM, New York, NY, USA, 9 pages. <https://doi.org/10.1145/3512290.3528721>

1 INTRODUCTION

Recurrent neural networks provide an efficient way of data processing in organic tissue. However, training artificial recurrent networks

Permission to make digital or hard copies of all or part of this work for personal or classroom use is granted without fee provided that copies are not made or distributed for profit or commercial advantage and that copies bear this notice and the full citation on the first page. Copyrights for components of this work owned by others than the author(s) must be honored. Abstracting with credit is permitted. To copy otherwise, or republish, to post on servers or to redistribute to lists, requires prior specific permission and/or a fee. Request permissions from permissions@acm.org.
GECCO '22, July 9–13, 2022, Boston, MA, USA

© 2022 Copyright held by the owner/author(s). Publication rights licensed to ACM.
ACM ISBN 978-1-4503-9237-2/22/07...\$15.00
<https://doi.org/10.1145/3512290.3528721>

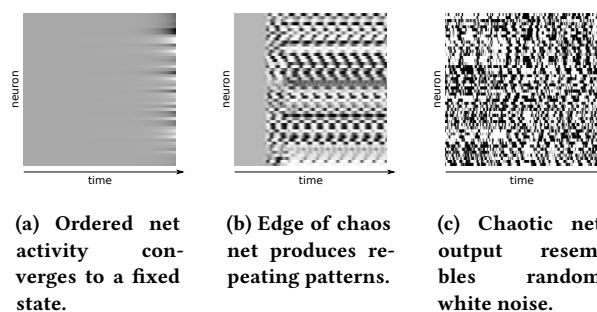


Figure 1: The states of three echo state networks tuned for ordered, edge of chaos and chaotic dynamics (left to right). Each column represents the activation of all its 50 reservoir neurons. The networks were driven by one positive input and the rest of the inputs were set to zero.

still poses a challenge [30] even though the artificial models are vastly simplified compared with their biological counterparts. In order to overcome the difficulty of training and avoid vanishing and exploding gradient problems, Jaeger[13] proposed a model called *Echo State Network* (ESN). The model uses a large recurrent reservoir which stays fixed throughout the whole lifetime of the network and, therefore, completely avoids the gradient propagation pitfalls. ESNs are especially useful for time series modelling [32]. In real-world applications, they have demonstrated promising results e.g., in financial markets [16][7], weather forecasting [16][28][37], microsleep detection [1] and many more.

ESNs are specified by a set of hyperparameters that define the behavior and properties of the network. Even though they are claimed to be robust against various hyperparameter changes [13], we will demonstrate that improper tuning of those hyperparameters can severely impact the network's performance. The most usual method of ESN hyperparameter tuning is a *grid search* [14][23][25][22], where the best hyperparameters are chosen from a predefined set of combinations. Unfortunately, this method may lead to underperforming networks and, therefore, questionable results when comparing different topologies or other architectural changes.

According to some authors (e.g., [26] [4]), ESNs tend to maximize their performance when their recurrent dynamics is close to the so-called *edge of chaos*. Unfortunately, networks in this regime are very sensitive to hyperparameter changes and even a small perturbation can turn a flawless network to a chaotic white noise generator (Figure 1). Besides the overall complicated hyperparameter space of a recurrent system, this nonlinear sensitivity adds in one more challenge that makes hyperparameter tuning difficult.

Contrary to e.g., *backpropagated* neural networks, the ESN training procedure is very fast. This fundamental property allows for various hyperparameter optimization techniques requiring thousands of *fitness* evaluations, which would be very impractical for traditional neural network models. With that in mind, we propose a tuning method based on an *Covariance Matrix Adaptation Evolution Strategy (CMA-ES)* [11] for continuous optimization, which has the potential to demonstrate the real possibilities of echo state networks.

One of the downsides of the proposed tuning algorithm are its computational demands. We need to run the full network evaluation thousands of times to make sure we converge to an optimum. For such a time consuming procedure to finish in a reasonable time, we have created a highly optimized C++ implementation of ESNs for graphical processors (GPU). Nevertheless, each of our many experiments still consumes tens of hours of computational time on a consumer-grade CPU and GPU.

The goal of the experiments presented in this paper is not to present a time-efficient method of ESN optimization, but to prove the existence of unexpected and performant parameter configurations difficult to find using a grid search or manual tuning. The experiments will compare the results of various ESN improvements found in literature with a properly tuned basic model. Narrowing the search space or reducing the required computational resources is left for future work.

2 RELATED WORK

One of the downsides of CMA-ES is its requirement of large number of function evaluations to be able to provide satisfying results. That is why its utilization in models with long evaluation times, such as deep neural networks, may be challenging. There are alternative approaches promising lower number of evaluations, usually with a performance trade-off. Some of the examples are Bayesian optimization [25][38][5], random search [3], gradient based methods [34], evolutionary algorithms [35][26][8], and even analytical approaches [20]. There are also attempts to speed up the CMA-ES itself by warm starting it using previous or transferred knowledge [29].

Despite the challenges, there has been multiple attempts to use CMA-ES for hyperparameter tuning of ESNs and neural networks in general. For instance, Loshchilov and Hutter [21] used CMA-ES for hyperparameter optimization of deep neural networks on handwritten digit recognition task. With sufficient number of evaluations and enough computational time, CMA-ES eventually outperformed state-of-the-art Bayesian methods. In a recent study, Liu and Zhang [19] employed CMA-ES specifically in echo state network hyperparameter optimization and reached similar results. However, even though their model outperformed other optimization approaches in the three tasks evaluated in the study, their approach had a few drawbacks preventing it from reaching state-of-the-art performance. First, only three hyperparameters were optimized, crucially restricting the network's possibilities. Second, the training data had only 1000 time steps, which seems inadequate for a reservoir of up to 1000 neurons (discussed in Section 6).

In our paper, the list is extended to eight hyperparameters, which on one hand provides more degrees of freedom, but on the other hand, the extended search space and its sensitivity pose a challenge

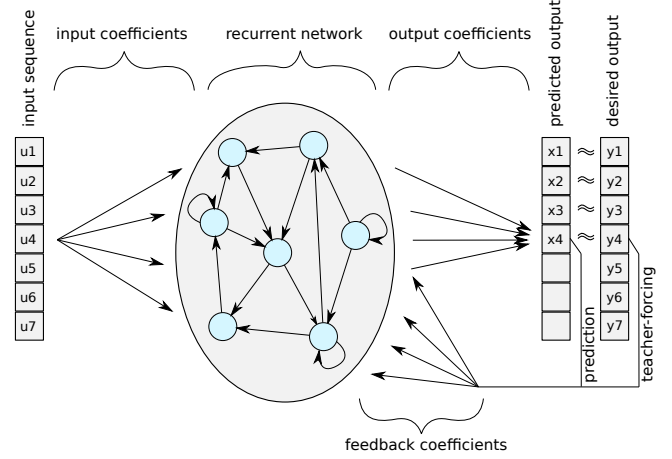


Figure 2: Echo state network overview.

for the optimizer. Furthermore, some hyperparameters require careful steps as their absolute value closes to zero while some prefer linear steps throughout their whole domain. To address the issue, we have transformed the search space of some parameters according to their needs.

3 METHODS

3.1 Echo State Networks

An echo state network (Figure 2) with n neurons as defined by Jaeger [13] consists of a *reservoir* with connectivity matrix $W \in \mathbb{R}^{n \times n}$, a vector of *input coefficients* denoted by $w_{in} \in \mathbb{R}^n$, a vector of *readout coefficients* denoted by $w_{out} \in \mathbb{R}^n$ and a vector of *feedback coefficients* denoted by $w_{fb} \in \mathbb{R}^n$. The activations of the neurons in the recurrent network in time t are denoted as $a(t) \in \mathbb{R}^n$, the input value as $u(t) \in \mathbb{R}$, the output value as $x(t) \in \mathbb{R}$ and the desired output as $y(t) \in \mathbb{R}$. The recurrence and the output are calculated as follows:

$$\begin{aligned} z(t) &= Wa(t-1) + w_{in}u(t) + w_{fb}x(t-1) + \mu_b, \\ a(t) &= (1 - \gamma)a(t-1) + \tanh(z(t)) \odot N_n(1, \epsilon^2), \\ x(t) &= a(t) \cdot w_{out}, \end{aligned}$$

where $z(t) \in \mathbb{R}^n$ are the raw potentials before being processed by tanh activation function, $\gamma \in \mathbb{R}$ is the leakage parameter, $\mu_b \in \mathbb{R}$ denotes the constant bias, \odot represents elementwise multiplication, $N_n(1, \epsilon^2) \in \mathbb{R}^n$ is a vector with each element drawn independently from *normal distribution* $N(1, \epsilon^2)$, and $\epsilon \in \mathbb{R}$ denotes the strength of the internal noise.

The reservoir matrix and the input and feedback coefficients are generated randomly and stay fixed. The output coefficients w_{out} are trained using linear regression so that the predicted sequence $x(t)$ and the desired output sequence $y(t)$ minimize their squared distance. Specifically, during the training, the network is driven by the training input sequence u with the desired output sequence y , both of length k . Let us define matrix $A \in \mathbb{R}^{k \times n}$ whose i -th row is the vector of activations $a(i)$. Afterwards, the least squares method

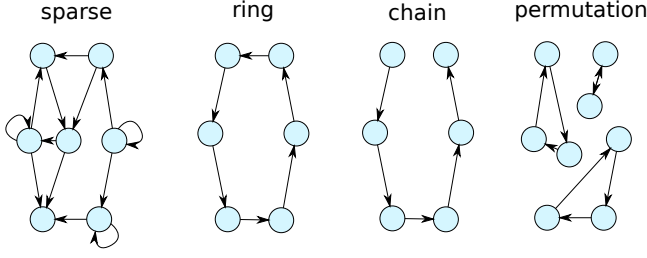


Figure 3: Common ESN topologies.

is used to find w_{out} as follows:

$$w_{out} = \arg \min_w \|Aw - y\|,$$

where $\|\cdot\|$ denotes the *Euclidean norm*.

During the training phase (i.e., before the initialization of w_{out}), the feedback connections are driven by the desired output sequence $y(t)$ and during the testing phase, the feedback connections use the network prediction $x(t)$. This process is known as teacher-forcing [13][22] and it is depicted in Figure 2.

3.2 Topologies

In our experiments, we compare four variants of the reservoir as depicted in Figure 3. The most common variant is called *sparse* topology. Its reservoir is a fully connected network where every edge has a probability $\alpha \in [0, 1]$ to be missing. This corresponds to a weight matrix W initialized from $N(\mu_{res}, \sigma_{res}^2)$ whose elements are set to zero with the probability α .

Another usual topology is called *chain*. It is created by numbering the neurons from 1 to n and connecting neuron i to neuron $i + 1$ while leaving the last neuron n disconnected. The corresponding weight matrix is shown in Equation 1.

$$\begin{bmatrix} 0 & \dots & \dots & 0 \\ w_1 & \ddots & & \vdots \\ \vdots & \ddots & \ddots & \vdots \\ 0 & \dots & w_n & 0 \end{bmatrix} \quad (1)$$

If the last neuron n connects back to neuron 1, it is called the *ring* topology. The reservoir matrix of the ring is similar to the chain reservoir, but it has a nonzero value w_{n+1} in its upper right element. Both the chain and ring topologies have been shown to have similar properties as the sparse topology with regard to memory capacity and some authors have suggested that the research should use those topologies as a baseline [31][25]. The last examined topology is called *permutation* and it is created by randomly shuffling the rows of the ring topology matrix. This operation effectively splits the long ring to a number of smaller rings of different lengths.

Some authors (e.g., [25]) use the same constant for all the nonzero connection weights in the ring, chain, and permutation topologies instead of generating the values from $N(\mu_{res}, \sigma_{res}^2)$ as is the case for the sparse topology (e.g., [9]). In other words, the reservoir matrix W can be expressed as λW_b , where W_b is a binary matrix and λ is the desired constant. During our experiments, we have avoided this restriction in order not to give an unfair advantage of

an extra degree of freedom to the sparse topology. All the weights are generated from $N(\mu_{res}, \sigma_{res}^2)$ and both μ_{res} and σ_{res} are part of the optimized hyperparameters. If favorable, the optimization algorithm can enforce the constant values by setting $\mu_{res} = \lambda$ and $\sigma_{res} = 0$.

It is worth noting that the sparse topology has $O(n^2)$ parameters where n is the number of neurons, whereas the ring, chain and permutation topologies have only $O(n)$ parameters. Analogously to other papers (e.g., [9] [31]), we compare topologies with the same number of neurons, not the same number of parameters.

3.3 CMA-ES

Covariance Matrix Adaptation Evolution Strategy (CMA-ES [11]) is a continuous optimization algorithm from a wide class of evolutionary strategies. The algorithm generates a population of candidate solutions, evaluates their fitness and estimates the natural gradient. Afterwards, it makes a step in the direction of the gradient in order to minimize the fitness. During the evolution, the algorithm adapts the covariance matrix from which it generates the population.

ESNs do not seem to have a single optimal set of hyperparameters, but instead, the parameters must be in a fragile balance. Therefore, CMA-ES is well suited for the task of ESN hyperparameter optimization as the covariance matrix captures the dependencies between individual hyperparameters and generates sensible candidates.

In our experiments, we use a modification called *active CMA-ES* [15], which updates its covariance matrix based on both successful and unsuccessful candidates, therefore avoiding unpromising parts of the search space. Thorough explanation of CMA-ES is beyond the scope of this paper, please refer to, e.g., the tutorial paper by Hansen [10] for more details.

3.4 Ordered and Chaotic Dynamics

Let us provide a brief informal description of chaotic and ordered dynamics. In an *ordered system*, a small perturbation of initial conditions tends to vanish with time. In a *chaotic system*, on the other hand, even the smallest perturbation amplifies and eventually leads to a very different behavior of the system.

Echo state networks depending on their hyperparameters can be anywhere between total order and absolute chaos (Figure 1). In between those two regimes, there lies a narrow band called the *edge of chaos*. Some authors claim that the ordered side of the edge of chaos is the setting where the echo state networks demonstrate the best performance and maximize various information theory measures [26][4].

For more details regarding the chaos theory and time series analysis in general, please refer to Sprott [33].

3.5 Benchmarks

The selected topologies will be optimized to maximize the performance on two univariate time series prediction benchmarks. Unfortunately, researchers have not yet converged to a single and easily comparable performance measure and even though there exist widely used benchmark tasks, many authors have developed their specific modification or parametrization. Unless specified otherwise, we will use the measures from Gallicchio and Micheli [9].

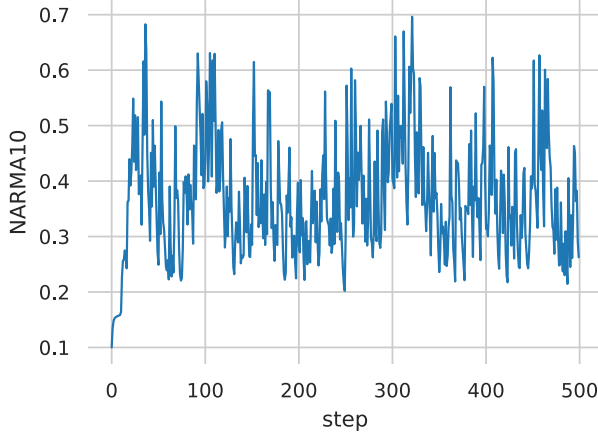


Figure 4: A possible realization of the NARMA10 sequence.

3.5.1 NARMA10. In the first task the network is driven by a random input sequence and its target is a *Non-linear Autoregressive Moving Average* of 10th order (NARMA10), i.e., a nonlinear combination of the last 10 inputs and outputs. Formally, the desired output sequence is defined as follows:

$$y(t+1) = 0.3y(t) + 0.05y(t) \sum_{i=0}^9 y(t-i) + 1.5u(t-10)u(t) + 0.1,$$

where $u(t)$ is the random input sequence generated from uniform distribution $U(0, 0.5)$ in time t and $y(t)$ is the desired output sequence in time t .

Recent research by Kubota et al. [18] identified that NARMA10 sequence has a significant probability of divergence. Even though it makes it an inconvenient comparison benchmark, it is still widely used in ESN literature, both historical and new. To prevent the divergence in our experiments, we check whether the generated NARMA10 sequences are bounded by $[-1, 1]$ and regenerate them otherwise. One possible realization of the NARMA10 sequence is demonstrated in Figure 4.

3.5.2 Mackey-Glass Equation. In the second benchmark, the network is driven by a sequence generated from *Mackey-Glass* equations (e.g., [13]) and its task is to predict the next value. The desired sequence is obtained by discretizing the following differential equation:

$$\frac{\delta u(t)}{\delta t} = \frac{0.2u(t-\tau)}{1+u(t-\tau)^{10}} - 0.1u(t)$$

where τ is a parameter of the equation, and δt is the discretization constant set to 0.1. Adopting the method from Jaeger [13], the discretization is approximated as:

$$u(t+1) = u(t) + \delta \left(\frac{0.2u(t-\frac{\tau}{\delta})}{1+u(t-\frac{\tau}{\delta})^{10}} - 0.1u(t) \right)$$

and the resulting sequence is subsampled by taking every tenth element. Furthermore, before feeding the values to the network, they are transformed to interval $[-1, 1]$ by $x \rightarrow \tanh(x-1)$ and the output of the network is transformed back to the original range by $x \rightarrow \operatorname{atanh}(x) + 1$. Throughout this paper, we use $\tau = 30$ and

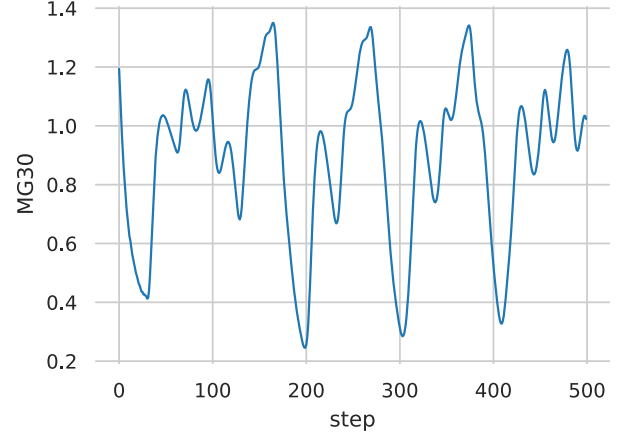


Figure 5: A possible realization of the MG30 sequence.

$\tau = 17$ and call the benchmarks MG30 and MG17 respectively. One possible realization of the MG30 sequence is demonstrated in Figure 5.

Unless specified otherwise, the performance of all tasks is measured using the *mean squared error* (MSE) of the desired and the predicted output sequences. In some experiments, we will be using *normalized mean squared error* (NMSE) defined as:

$$NMSE = \sum_{t=1}^N \frac{(y(t) - x(t))^2}{N\sigma^2},$$

where $y(t)$ is the desired output sequence and $x(t)$ is the predicted sequence, N is the length of the sequences, and σ^2 is the variance of the desired output sequence. And the last measure is *normalized root mean squared error* defined as:

$$NRMSE = \sqrt{NMSE}.$$

4 EXPERIMENTAL ENVIRONMENT

The hyperparameters of each reservoir topology are optimized so that the instantiated network maximizes its performance on one of the benchmark tasks. Similarly to [9], the experiment uses ESNs with 500 reservoir neurons, regardless of the topology. The reservoir weights are generated from normal distribution $N(\mu_{res}, \sigma_{res}^2)$, feedback weights from uniform distribution $U(-\omega_{fb}, \omega_{fb})$, and input weights from $U(-\omega_{in}, \omega_{in})$. Every weight in the reservoir will be set to zero with the probability of β . The optimized hyperparameters are reservoir parameters σ_{res} and μ_{res} , input weight spread ω_{in} , feedback weight spread ω_{fb} , sparsity α , leakage γ , bias μ_b and internal noise ϵ . Parameters σ_{res} and ϵ are optimized in logarithmic space via $x \mapsto e^{-50x}$. Parameters μ_{res} , ω_{in} , ω_{fb} , and μ_b are optimized in square root space via $x \mapsto 2x|x|$ to make more cautious steps in the close proximity to zero. The hyperparameters for every topology are optimized ten times over and in each of those trials, the best encountered network is evaluated a hundred times using a freshly generated inputs and outputs. The trial with the best mean performance is reported.

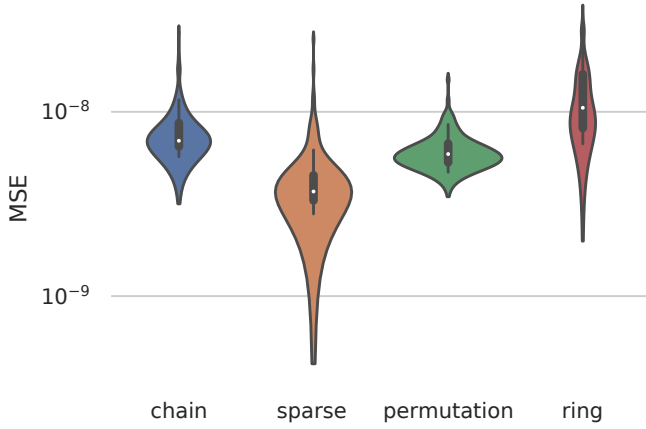


Figure 6: MSE on the NARMA10 task.

The starting parameters do not seem to be that important as long as the corresponding network is not overly chaotic or overly stable and the optimizer can detect an improving gradient. We handpicked those to $\sigma_{res} = \frac{1}{2k}$, where k is the average number of neuron inputs, $\omega_{in} = 0.02$, $\omega_{fb} = 0$, $\beta = 0.1$, $\gamma = 0.9$, $\mu_b = 0$, and $\epsilon = 4.5e^{-5}$. The initial sigma for CMA-ES is set to 0.05 except for σ_{res} and ω_{fb} where we use 0.01. The optimization is bounded to interval $[-1.1; 1.1]$ (before the search space transformation) and limited to 5000 evaluations which is more than sufficient to converge for all the tested combinations of topologies and benchmark tasks.

The initial neuron activation is set to zero and the first 1000 steps are used as a washout period to eliminate the effect of state initialization. The subsequent 5000 steps are used for linear regression training and the last 5000 steps are used for performance test.

In a few experiments where performance comparison may be unclear, we perform significance testing using Welch's t-test with statistical significance level of 0.05.

5 RESULTS

The results for the NARMA10 task are shown in Figure 6 and Table 1. The sparse topology slightly outperformed all the other topologies ($p < 0.05$). The presented results differ by multiple orders of magnitude from e.g. Gallicchio and Micheli [9], who reached NARMA10 $\approx 10^{-4} \pm 10^{-5}$, MG17 $\approx 10^{-9} \pm 10^{-10}$, and MG30 $\approx 10^{-8} \pm 10^{-9}$. The parameters in the aforementioned work were tuned manually and the sparse topology ended up as the worst of the four.

Most of the difference from [9] is caused by the fact that the authors have not used feedback connections, which even though difficult to tune manually [17] can staggeringly improve the results in autoregressive tasks, e.g., NARMA10. Furthermore, ESNs with feedback achieve universal computational capabilities [24]. Note that there is no benefit in using feedback connections for tasks where the input and the desired output sequences are equal and only shifted by one step (e.g., our variants of MG17 and MG30). In those tasks, the network is already fed by the desired output and

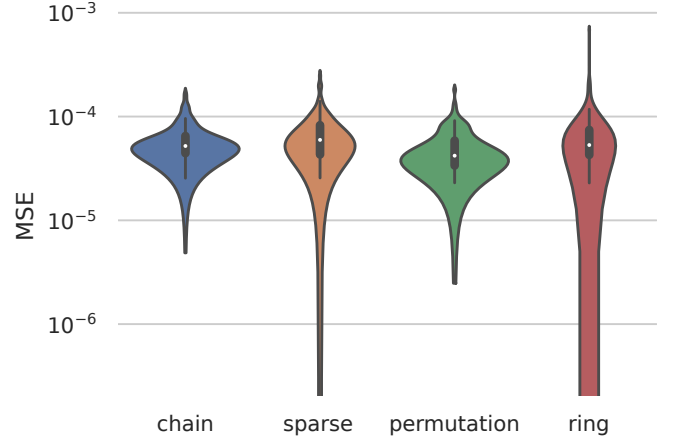


Figure 7: MSE on the NARMA10 task for networks without feedback connections.

feeding its own prediction through feedback would only introduce a new kind of noise for which the network has not been trained¹.

To demonstrate the effect of feedback connections, the NARMA10 experiment was repeated without the feedback connections as well and the results can be found in Figure 7 and Table 2. The results are orders of magnitude worse compared to the results with feedback connections, however, there is still a significant improvement compared to the results presented in [9] and all of the topologies still perform similarly. The authors in [9] propose a hypothesis that permutation, ring and chain topologies provide better performance than the sparse topology on NARMA10, MG17 and MG30 benchmarks. Our results oppose the hypothesis by properly tuning the hyperparameters of the sparse topology. Furthermore, the CMA-ES results on the aforementioned tasks surpassed even multi-layered *Deep ESN* results from the discussed paper.

With a slight modification of the experiments, the results can be compared also with *swarm optimization* method by Wang and Yan [35]. In NARMA10 task with a network counting 500 neurons, the CMA-ES procedure reached NMSE $5.2 \times 10^{-7} \pm 1.95 \times 10^{-4}$ compared to 0.0346 reported in [35]. In MG84-17 task, the NRMSE₈₄ is $1.28 \times 10^{-4} \pm 4.8 \times 10^{-5}$ for the CMA-ES and 1.4×10^{-3} for swarm optimization. It is worth mentioning that the authors have reached the results in a fraction of function evaluations compared to our method, however, the progress of the swarm optimization stalled after ≈ 150 iterations.

Further comparison can be done e.g., with the benchmark variants by Cerina et al. [5]. Adapting the measures defined in the paper, our method reached NRMSE in NARMA10 $\approx 99.928\%$, and MG10-17 $\approx 99.993\%$. The presented results were NARMA10 $\approx 90.647\%$ and MG10-17 $\approx 99.98\%$. It should be pointed out that the goal of [5] was to create a constrained network for devices with limited computational and memory resources, not to solely maximize the performance measures.

In comparison with another paper discussing different topologies by Čerňanský and Tiňo[6], our CMA-ES procedure reached

¹During the training, the network is fed by the desired output using the teacher-forced signal.

topology	NARMA10	MG17	MG30
sparse	$4.67 \times 10^{-9} \pm 3.0 \times 10^{-9}$	$1.27 \times 10^{-13} \pm 1.8 \times 10^{-14}$	$6.74 \times 10^{-10} \pm 1.5 \times 10^{-10}$
permutation	$6.34 \times 10^{-9} \pm 1.6 \times 10^{-9}$	$2.40 \times 10^{-13} \pm 6.0 \times 10^{-14}$	$5.06 \times 10^{-10} \pm 8.0 \times 10^{-11}$
chain	$8.18 \times 10^{-9} \pm 3.2 \times 10^{-9}$	$1.70 \times 10^{-13} \pm 2.8 \times 10^{-14}$	$5.54 \times 10^{-10} \pm 8.4 \times 10^{-11}$
ring	$1.28 \times 10^{-8} \pm 5.9 \times 10^{-9}$	$2.28 \times 10^{-13} \pm 8.6 \times 10^{-14}$	$6.89 \times 10^{-10} \pm 1.1 \times 10^{-10}$

Table 1: The MSE results of the four tested topologies on NARMA10, MG17 and MG30 benchmarks

topology	NARMA10 (no feedback)
sparse	$7.0 \times 10^{-5} \pm 3.9 \times 10^{-5}$
permutation	$5.1 \times 10^{-5} \pm 2.6 \times 10^{-5}$
chain	$5.9 \times 10^{-5} \pm 2.6 \times 10^{-5}$
ring	$7.1 \times 10^{-5} \pm 7.2 \times 10^{-5}$

Table 2: The MSE results of the four tested topologies without feedback connections on NARMA10 benchmarks.

topology	NARMA10
sparse	$3.08 \times 10^{-4} \pm 1.7 \times 10^{-4}$
permutation	$1.19 \times 10^{-3} \pm 7.6 \times 10^{-4}$
chain	$1.49 \times 10^{-3} \pm 9.6 \times 10^{-4}$
ring	$1.79 \times 10^{-3} \pm 2.6 \times 10^{-3}$

Table 3: The NMSE results of the four tested topologies on NARMA10 variant by Rodan and Tino.

MG17 MSE = $6.49 \times 10^{-16} \pm 3.99 \times 10^{-17}$ and NARMA10 MSE = $1.4 \times 10^{-4} \pm 7.4 \times 10^{-5}$ versus the best presented results in the paper MG17 MSE = $9.82 \times 10^{-16} \pm 9.02 \times 10^{-17}$ and NARMA10 MSE = $8.4 \times 10^{-4} \pm 8.4 \times 10^{-5}$. Even though the results presented in [6] are slightly surpassed by our method, the authors have reached impressive performance simply by dividing the reservoir matrix by its largest eigenvalue. This scaling technique transforms the reservoir to be close to the edge of chaos dynamics.²

Our method is also superior to the topology comparison results by Rodan and Tino[31]. The authors of this paper were one of the first to introduce the idea of minimum complexity echo state networks, specifically variants of the ring topology. They conclude that the proposed simple topologies offer a similar performance to the sparse topology while being easier to construct and easier to train. We managed to reproduce and significantly improve their results in NARMA10 task (reported NMSE ≈ 0.04) with reservoir size 200 for the chain, ring, and permutation topologies. However, the sparse topology significantly outperformed all of them ($p < 0.05$). See Figure 8 and Table 3.

Holzmann and Hauser[12] experimented not with a topology, but with the neuron itself. They designed a neuron with band pass filter and a new kind of delay&sum readout. The results were compared with a plain ESN on a more difficult version of the NARMA10 benchmark with lag variable τ . In their paper, the plain ESN error

²It should be noted that the authors use a large network of 1000 neurons for the MG17 task and even better results can be achieved by increasing the training sequence length.

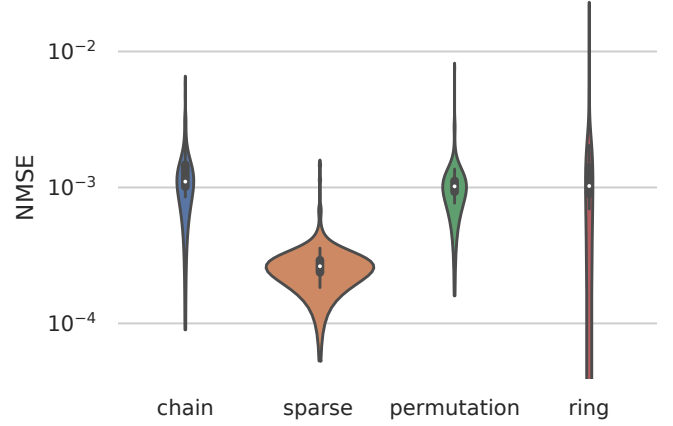


Figure 8: NMSE on the NARMA10 variant by Rodan and Tino [31].

reservoir size	CMA-ES	GA
200	0.12 ± 0.005	0.15 ± 0.005
400	0.02 ± 0.001	0.09 ± 0.013

Table 4: The NMSE results on the NARMA30 task by Dale [8].

quickly soars as the τ increases and for $\tau > 2$ its NRMSE reaches values up to 0.8, while their improved version of the network stays just slightly above 0.4. We have reproduced their results with our CMA-ES optimization and the plain ESN results outperformed all of the modifications. For $\tau = 2$, NRMSE in the NARMA10 task was 0.36 ± 0.01 and for $\tau = 4$, it was 0.38 ± 0.01 .

Finally, the CMA-ES results with plain ESN are superior to a hierarchy of ESNs optimized by a genetic algorithm on NARMA30 task by Dale [8] with results presented in Table 4.

6 DISCUSSION

According to the results, plain ESN with the sparse reservoir topology can achieve extraordinary performance as long as it has been properly tuned. Unfortunately, many authors appear to underestimate hyperparameter optimization and compare their innovations with subpar ESN instances. To their defense, manual parameter tuning is very difficult and grid search cannot cover the small nuances created by fragile recurrent dynamics.

Let us demonstrate an example. Taking the hyperparameters of one of the best performing sparse networks on the NARMA10

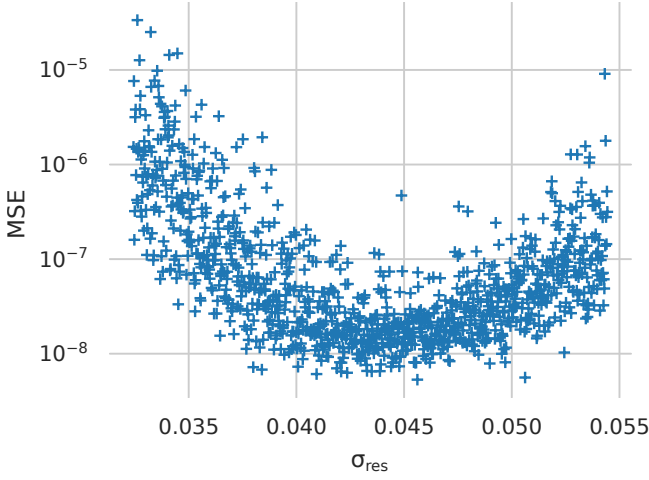


Figure 9: MSE versus σ_{res} in a narrow range around the optimum.

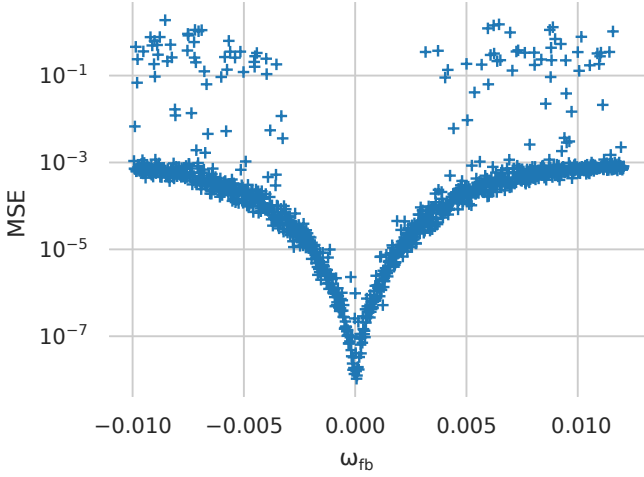


Figure 10: MSE versus ω_{fb} on a coarse grid.

benchmark, let us plot a few perturbations close to the optimal σ_{res} in Figure 9. The optimal interval is very narrow, for instance, when $1e-2$ is subtracted from the σ_{res} , the error on the NARMA10 task soars by more than one order of magnitude.

To further demonstrate the pitfalls of hyperparameter tuning, Figure 10 shows a scatter plot with the effect of small perturbations of ω_{fb} . The required grid density would need to be $\approx 1 \times 10^{-3}$ to recognize the depicted pattern. By the shape of the plot, one could assume that feedback weights are inadequate for the task as the error is minimized when ω_{fb} is set to zero. Unfortunately, if we plot a detail with even denser grid of step size at most $\approx 1 \times 10^{-5}$ as shown in Figure 11, we can clearly see that feedback weights are necessary. However they need to be set to a very narrow range between 5×10^{-5} and 1×10^{-4} .

During our experiments, we have encountered situations where this steep decrease in performance in the vicinity of zero blocked the CMA-ES algorithm from changing the sign of the optimized

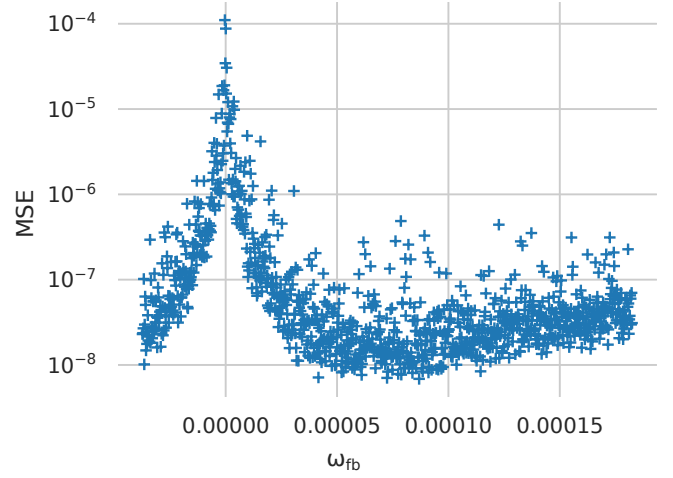


Figure 11: MSE versus ω_{fb} in a narrow range around the optimum.

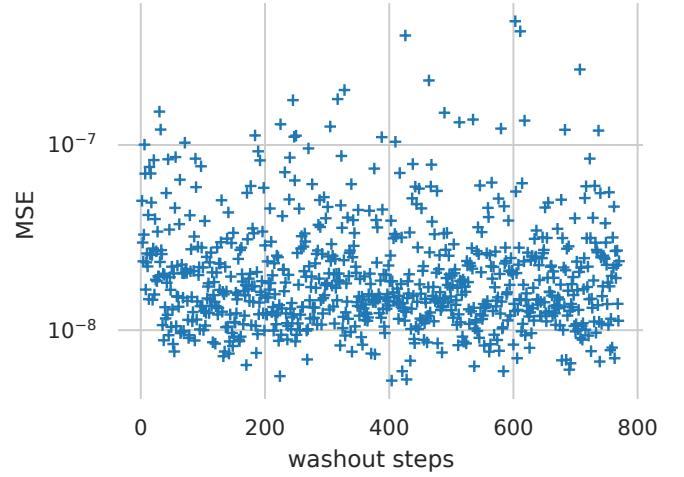


Figure 12: MSE versus the number of washout steps.

variable. This poses a problem especially in later stages of the evolution, when the spread of the candidates becomes smaller. We recommend running the optimization multiple times to increase the probability of obtaining the correct sign for all the variables.

Considering the necessity of a very dense hyperparameter grid and the fact that there are eight parameters to be optimized, grid search becomes nearly impossible due to the *curse of dimensionality*. What is convenient about the restricted topologies, such as ring or chain, is that each neuron has a smaller number of input connections and the network has a stronger tendency to stay in the ordered regime. Therefore, the range of hyperparameters in which the network provides reasonable performance dilates, and thus becomes easier to optimize manually or via grid search.

One thing we have seen to vary in the literature are the lengths of the washout and training sequences. A rule of thumb is to have at least as many washout steps as there are neurons in the network. The necessary number of washout steps may depend on the

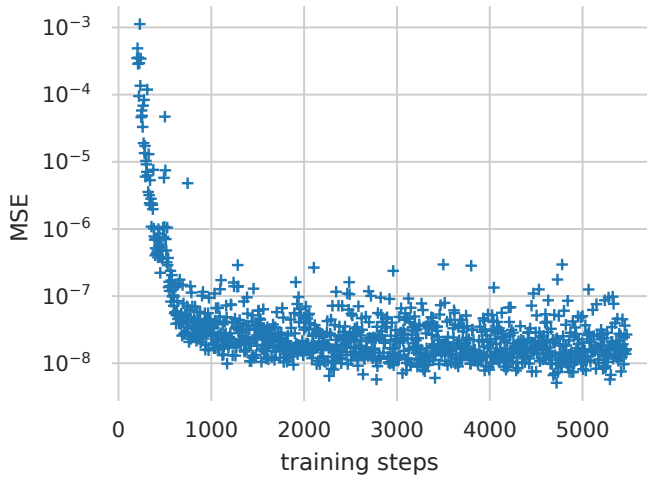


Figure 13: MSE versus the number of training steps.

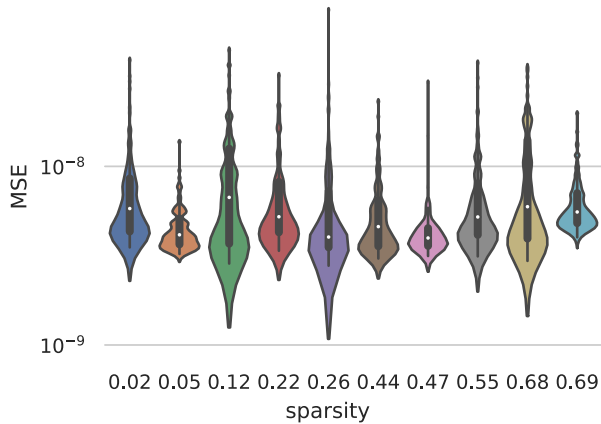


Figure 14: The performance of the best individuals from ten independent evolutionary runs on the NARMA10 task plotted against their sparsity.

topology of the network (specifically its diameter) and its dynamics, especially the reach of its memory. For instance, in our NARMA10 network, anything above 100 seems sufficient (Figure 12). What is more demanding is the train sequence length. As depicted in Figure 13 our network requires at least 4000 training steps to reach its full potential.

Another noteworthy observation is that the sparsity parameter β in the sparse topology did not seem to play an important role and the best found sparse networks balanced other parameters accordingly without a noticeable performance loss (Figure 14). However, it should be pointed out that none of the ten networks has sparsity above 70%. Nonetheless, the likely reason is that there is simply no gradient pushing the sparsity higher from the initial value of 10% and the sparsity parameter merely performs a random walk around its origin. Naturally, the sparsity plays much more important role

in the circle and chain topologies, where each dropped connection creates a new disconnected component. The sparsity of the best individuals with those two topologies has always been optimized out to zero.

During our experiments, we have encountered many extreme values, especially while evaluating the ring and chain topologies. One explanation could be that those topologies may be prone to generating a subpar reservoir instance, e.g., a ring where a few connections gets a very low weight and, consequently, create a bottleneck not passing the data further in the ring. Taking this property into account when using ESNs in practice, one should always train multiple instances and use the best performing one.

7 CONCLUSION

We have investigated the challenge of hyperparameter tuning in echo state networks with multiple different topologies.

Our results suggest that restricted topologies, such as chain, ring and permutation do not provide any significant performance edge over a plain sparse network with properly tuned hyperparameters and even underperform in some of the evaluated tasks.

We argue that grid search is not a proper way to tune hyperparameters because a small perturbation can cause large differences in performance and the grid would need to be impractically dense. This is especially true for networks close to the edge of chaos.

Results of papers comparing various ESN innovations, such as topologies, are questionable without a proper hyperparameter tuning. For trustworthy evaluation of novelties in ESNs, we propose the usage of CMA-ES as a robust, yet computationally intensive tool to tune the hyperparameters.

To the best of our knowledge, the proposed results form a new baseline for echo state networks in NARMA10, MG17, and MG30 benchmarks for ESNs with the corresponding number of neurons.

We have implemented a highly optimized C++ framework for ESN optimization with GPU support. The source code will be publicly available on our GitHub page [27] under permissive license including the configuration for all the evaluated experiments.

8 CITATIONS AND BIBLIOGRAPHIES

ACKNOWLEDGMENTS

This research was supported by Charles University grant SVV-260588 and GA UK project number 1578717. Computational resources were supplied by the project “e-Infrastruktura CZ” (e-INFRA CZ LM2018140) supported by the Ministry of Education, Youth and Sports of the Czech Republic. We thank the authors of ArrayFire [36] and libcmaes [2] software packages for sharing their hard work under open source licences.

REFERENCES

- [1] Sudhanshu Ayyagari, Richard Jones, and Stephen Waddell. 2015. Optimized echo state networks with leaky integrator neurons for EEG-based microsleep detection. *Conference proceedings: Annual International Conference of the IEEE Engineering in Medicine and Biology Society*. 2015, 3775–3778. <https://doi.org/10.1109/EMBC.2015.7319215>
- [2] Emmanuel Benazera. 2022. Libcmaes - A multithreaded C++11 implementation of algorithms of the CMA-ES family. <https://github.com/CMA-ES/libcmaes>
- [3] James Bergstra and Yoshua Bengio. 2012. Random Search for Hyper-Parameter Optimization. *Journal of Machine Learning Research* 13, 10 (2012), 281–305. <http://jmlr.org/papers/v13/bergstra12a.html>

- [4] Nils Bertschinger and Thomas Natschl ger. 2004. Real-Time Computation at the Edge of Chaos in Recurrent Neural Networks. *Neural computation* 16, 7 (2004), 1413–1436.
- [5] Luca Cerina, Marco Santambrogio, Giuseppe Franco, Claudio Gallicchio, and Alessio Micheli. 2020. EchoBay: Design and Optimization of Echo State Networks under Memory and Time Constraints. *ACM Transactions on Architecture and Code Optimization* 17 (08 2020), 1–24. <https://doi.org/10.1145/3404993>
- [6] Michal  ernansk y and Peter Ti o. 2008. Predictive Modeling with Echo State Networks. In *Artificial Neural Networks - ICANN 2008*, V ra K rkov , Roman Neruda, and Jan Koutn k (Eds.). Springer Berlin Heidelberg, Berlin, Heidelberg, 778–787.
- [7] Emanuele Crisostomi, Claudio Gallicchio, Alessio Micheli, Marco Raugi, and Mauro Tucci. 2015. Prediction of the Italian electricity price for smart grid applications. *Neurocomputing* 170 (06 2015). <https://doi.org/10.1016/j.neucom.2015.02.089>
- [8] Matthew Dale. 2018. Neuroevolution of Hierarchical Reservoir Computers. In *Proceedings of the Genetic and Evolutionary Computation Conference* (Kyoto, Japan) (GECCO '18). Association for Computing Machinery, New York, NY, USA, 410–417. <https://doi.org/10.1145/3205455.3205520>
- [9] Claudio Gallicchio and Alessio Micheli. 2019. Reservoir Topology in Deep Echo State Networks. In *Artificial Neural Networks and Machine Learning – ICANN 2019: Workshop and Special Sessions*, Igor V. Tetko, V ra K rkov , Pavel Karpov, and Fabian Theis (Eds.). Springer International Publishing, Cham, 62–75.
- [10] Nikolaus Hansen. 2016. The CMA Evolution Strategy: A Tutorial. *ArXiv abs/1604.00772* (2016).
- [11] Nikolaus Hansen and Andreas Ostermeier. 2001. Completely derandomized self-adaptation in evolution strategies. *Evolutionary computation* 9, 2 (2001), 159–195. <https://doi.org/10.1162/106365601750190398>
- [12] Georg Holzmann and Helmut Hauser. 2009. Echo state networks with filter neurons and a delay and sum readout. *Neural networks : the official journal of the International Neural Network Society* 23 (08 2009), 244–56. <https://doi.org/10.1016/j.neunet.2009.07.004>
- [13] Herbert Jaeger. 2001. The “echo state” approach to analysing and training recurrent neural networks-with an erratum note’. *Bonn, Germany: German National Research Center for Information Technology GMD Technical Report* 148 (01 2001).
- [14] Herbert Jaeger. 2002. *Tutorial on training recurrent neural networks, covering BPPT, RTRL, EKF and the “echo state network” approach*. Vol. 5. GMD-Forschungszentrum Informationstechnik Bonn.
- [15] G.A. Jastrebski and D.V. Arnold. 2006. Improving Evolution Strategies through Active Covariance Matrix Adaptation. In *2006 IEEE International Conference on Evolutionary Computation*. 2814–2821. <https://doi.org/10.1109/CEC.2006.1688662>
- [16] Taehwan Kim and Brian King. 2020. Time series prediction using deep echo state networks. *Neural Computing and Applications* 32 (12 2020). <https://doi.org/10.1007/s00521-020-04948-x>
- [17] Danil Koryakin, Johannes Lohmann, and Martin Butz. 2012. Balanced echo state networks. *Neural networks : the official journal of the International Neural Network Society* 36C (09 2012), 35–45. <https://doi.org/10.1016/j.neunet.2012.08.008>
- [18] Tomoyuki Kubota, Kohei Nakajima, and Hirokazu Takahashi. 2019. Dynamical Anatomy of NARMA10 Benchmark Task. *ArXiv abs/1906.04608* (2019).
- [19] Kai Liu and Jie Zhang. 2020. Nonlinear process modelling using echo state networks optimised by covariance matrix adaption evolutionary strategy. *Computers & Chemical Engineering* 135 (2020), 106730. <https://doi.org/10.1016/j.compchemeng.2020.106730>
- [20] Lorenzo Livi, Filippo Maria Bianchi, and Cesare Alippi. 2017. Determination of the Edge of Criticality in Echo State Networks Through Fisher Information Maximization. *IEEE Transactions on Neural Networks and Learning Systems* 29 (01 2017), 1–12. <https://doi.org/10.1109/TNNLS.2016.2644268>
- [21] Ilya Loshchilov and Frank Hutter. 2016. CMA-ES for Hyperparameter Optimization of Deep Neural Networks. *CoRR abs/1604.07269* (2016). <http://arxiv.org/abs/1604.07269>
- [22] Mantas Luko ev cius. 2012. *A Practical Guide to Applying Echo State Networks*. Springer Berlin Heidelberg, Berlin, Heidelberg, 659–686. https://doi.org/10.1007/978-3-642-35289-8_36
- [23] Mantas Luko ev cius and Herbert Jaeger. 2009. Jaeger, H.: Reservoir computing approaches to recurrent neural network training. *Computer Science Review* 3, 127–149. *Computer Science Review* 3 (08 2009), 127–149. <https://doi.org/10.1016/j.cosrev.2009.03.005>
- [24] Wolfgang Maass, Prashant Joshi, and Eduardo D. Sontag. 2005. Principles of Real-Time Computing with Feedback Applied to Cortical Microcircuit Models. In *Proceedings of the 18th International Conference on Neural Information Processing Systems* (Vancouver, British Columbia, Canada) (NIPS'05). MIT Press, Cambridge, MA, USA, 835–842.
- [25] Jacob Reinier Maat, Nikos Gianniotis, and Pavlos Protopoulos. 2018. Efficient Optimization of Echo State Networks for Time Series Datasets. In *2018 International Joint Conference on Neural Networks (IJCNN)*. 1–7. <https://doi.org/10.1109/IJCNN.2018.8489094>
- [26] Filip Matzner. 2017. Neuroevolution on the Edge of Chaos. In *Proceedings of the Genetic and Evolutionary Computation Conference* (Berlin, Germany) (GECCO '17). Association for Computing Machinery, New York, NY, USA, 465–472. <https://doi.org/10.1145/3071178.3071292>
- [27] Filip Matzner. 2022. High-performance Echo State Network simulation, optimization and visualization in modern C++. <https://github.com/FloopCZ/echo-state-networks>
- [28] Patrick McDermott and Christopher Wikle. 2018. Deep echo state networks with uncertainty quantification for spatio-temporal forecasting. *Environmetrics* 30 (12 2018). <https://doi.org/10.1002/env.2553>
- [29] Masahiro Nomura, Shuhei Watanabe, Youhei Akimoto, Yoshihiko Ozaki, and Masaki Onishi. 2020. Warm Starting CMA-ES for Hyperparameter Optimization. *CoRR abs/2012.06932* (2020). [arXiv:2012.06932](https://arxiv.org/abs/2012.06932)
- [30] Razvan Pascanu, Tomas Mikolov, and Yoshua Bengio. 2013. On the Difficulty of Training Recurrent Neural Networks. In *Proceedings of the 30th International Conference on International Conference on Machine Learning - Volume 28* (Atlanta, GA, USA) (ICML '13). JMLR.org, III–1310–III–1318.
- [31] Ali Rodan and Peter Tino. 2011. Minimum Complexity Echo State Network. *IEEE Transactions on Neural Networks* 22, 1 (2011), 131–144. <https://doi.org/10.1109/TNN.2010.2089641>
- [32] Benjamin Schrauwen, David Verstraeten, and Jan Campenhout. 2007. An overview of reservoir computing: Theory, applications and implementations. *Proceedings of the 15th European Symposium on Artificial Neural Networks*, 471–482.
- [33] J.C. Sprott. 2003. *Chaos and Time-series Analysis*. Oxford University Press. <https://sprott.physics.wisc.edu/chaostsa/>
- [34] Luca Thiede and Ulrich Parlitz. 2019. Gradient based hyperparameter optimization in Echo State Networks. *Neural Networks* 115 (03 2019). <https://doi.org/10.1016/j.neunet.2019.02.001>
- [35] Heshan Wang and Xuefeng Yan. 2015. Optimizing the echo state network with a binary particle swarm optimization algorithm. *Knowledge-Based Systems* 86 (09 2015), 182–193. <https://doi.org/10.1016/j.knsys.2015.06.003>
- [36] Pavan Yalamanchili, Umar Arshad, Zakiuddin Mohammed, Pradeep Garigipati, Peter Entschew, Brian Kloppenborg, James Malcolm, and John Melonakos. 2022. ArrayFire - A high performance software library for parallel computing with an easy-to-use API. <https://github.com/arrayfire/arrayfire>
- [37] Meng-Hua Yen, Ding-Wei Liu, Yi-Chia Hsin, Chu-En Lin, and C.L. Chen. 2019. Application of the deep learning for the prediction of rainfall in Southern Taiwan. *Scientific Reports* 9 (09 2019), 1–9. <https://doi.org/10.1038/s41598-019-49242-6>
- [38] Jan Yperman and Thijs Becker. 2016. Bayesian optimization of hyper-parameters in reservoir computing. *ArXiv abs/1611.05193* (2016).